NANO LETTERS

2004
Vol. 4, No. 5
905−909

Rewritable Memory by Controllable Nanopatterning of DNA

Jong-Shik Shin[†] and Niles A. Pierce*[,†,‡]

Department of Bioengineering and Department of Applied and Computational Mathematics, California Institute of Technology, Pasadena, California 91125

Received March 3, 2004; Revised Manuscript Received March 26, 2004

ABSTRACT

Fabricating a nanostructure capable of reversibly patterning molecules is a fundamental goal within nanotechnology, underlying diverse processes such as information storage, scaffold-assisted assembly, and molecular transport. Here, we describe a DNA scaffold supporting a one-dimensional array of independently and reversibly addressable sites at 7 nm spacing. As a proof-of-concept, we demonstrate robust functioning of the device as rewritable memory. The bit state of each address is controlled by specific DNA strands with external readout provided by fluorescence measurements.

Autonomous bottom-up fabrication based on molecular recognition[1] is a conceptually attractive and potentially powerful approach to engineering structures and devices at the molecular scale. Molecular building blocks in a bottom-up approach must contain structural information that forces components to assemble and align without external manipulation. DNA is a versatile construction material that can be programmed to self-assemble into nanoscale structures based on specific complementarity between bases;[2−4] it has been used to build branched structures,[5,6] two-dimensional lattices,[7−9] and cyclic nanomechanical devices,[10−13] to create computational libraries of noninteracting strands and perform logical operations,[14−18] and to serve as a template for tethering nanoparticles.[19,20] Of particular interest are recent advances in cycling DNA nanostructures between two stable states through the addition of auxiliary DNA fuel strands.[10,11,13] To date, construction of DNA nanodevices that allow reversible and specific control over multiple states remains challenging.

The present objective is to develop an approach to controllable nanopatterning by designing a DNA array that can be used to reversibly tether molecules. The construction of dynamically addressable arrays combines several challenges that have been examined individually in previous DNA design efforts: Addresses must be ordered (as with a lattice[7]), specifically bindable (as with computational strand libraries[16]), and reversibly bindable (as with cyclic mechanical devices[10]). Here, we consider rewritable information storage as a particular application of controllable nanopatterning, using DNA to construct a prototype memory device with three independent addresses capable of representing eight states. Information storage in this format is expected to be compatible with use in synthetic circuits designed for biological information processing.[21]

The memory device is composed of five single-stranded oligonucleotides (D) with sequences shown in Figure 1. Stoichiometric mixing of the strands leads to a self-assembled structure carrying three addressable branches (see state 000 in Figure 2) that can be used to represent 2^3 memory states. The branches are separated by 20-bp scaffold helices leading to 7 nm spacing. The addressable branches are composed of 3-base spacers and 18-base sequences complementary to one of three writing strands (W). The structure of the memory device bears a superficial resemblance to 'frayed wires'[22] that self-assemble based on G-tetrad formation, but differs fundamentally in the specificity associated with both the scaffold assembly and the addressable branches.

The writing and erasing processes are depicted in Figure 2. Each W strand flips the corresponding address from a randomly coiled single-stranded "off" state to a linear double-stranded "on" state by forming a new 18-bp duplex. The 10-base overhang of each W strand, which dangles from the end of the 18-bp duplex, serves as a nucleation site for hybridization with the corresponding perfectly complementary erasing strand (E). The E strand strips off a cognate W strand from an "on" address, leading to a duplex waste product and resetting the address to the "off" state. Independent writing and erasing processes are specifically controlled by different sequence designs for the address branches and the overhangs of W strands. The writing process and erasure nucleation events are driven by the free-energy reduction resulting from incremental base-pairing.

* Corresponding author. 165 Broad (MC 114-96), California Institute of Technology, 1200 E. California Bl., Pasadena, CA 91125. E-mail: niles@caltech.edu. Tel: 626-395-8086. Fax: 626-395-8845.
[†] Department of Bioengineering.
[‡] Department of Applied and Computational Mathematics.

10.1021/nl049658r CCC: $27.50
Published on Web 04/13/2004

Device strands (D)

D1 5′-GCTGGTCTGGCACTAGGTGGACATCTAAGGACTACACTGGA-3′

D2 5′-GTGAATCGAAACTGTACCAATCCCTGCTTCGTCGCTTGTCACCACCTAGTGCCAGACCAGC-3′

D3 5′-TGACAAGCGACGAAGCAGGGTCAACGGTTGCAGCCAATGCTCTATCTCATTCCTCGGTCTA-3′

D4 5′-TATGTATCATCGGAGCGTGATGCACGATACGCATTGGCTGCAACCGTTGA-3′

D5 5′-GTATCGTGCATCACGCTCCGATGATACATA-3′

Writing strands (W)

W1 5′-*TACTCGACCT*TCCAGTGTAGTCCTTAGA-3′

W2 5′-GGTACAGTTTCGATTCAC*TCAACGGAGT*-3′

W3 5′-*TTACCTGACG*TAGACCGAGGAATGAGAT-3′

Figure 1. DNA sequences for the device strands (D) and writing strands (W). Sequences of D1, D2, and D3 consist of a scaffold segment, a 3-base spacer (in black) and an address segment (underlined), whereas D4 and D5 have only scaffold segments. Each scaffold segment of the D strands has a complementary counterpart of matching color in another D strand that forms the structural basis for the device. Each W strand contains an 18-base section complementary to the corresponding address sequence of the same color (e.g., W1 to D1) and an italicized 10-base overhang for nucleation with the corresponding E strand, which is a perfect complement (e.g., E1 to W1).

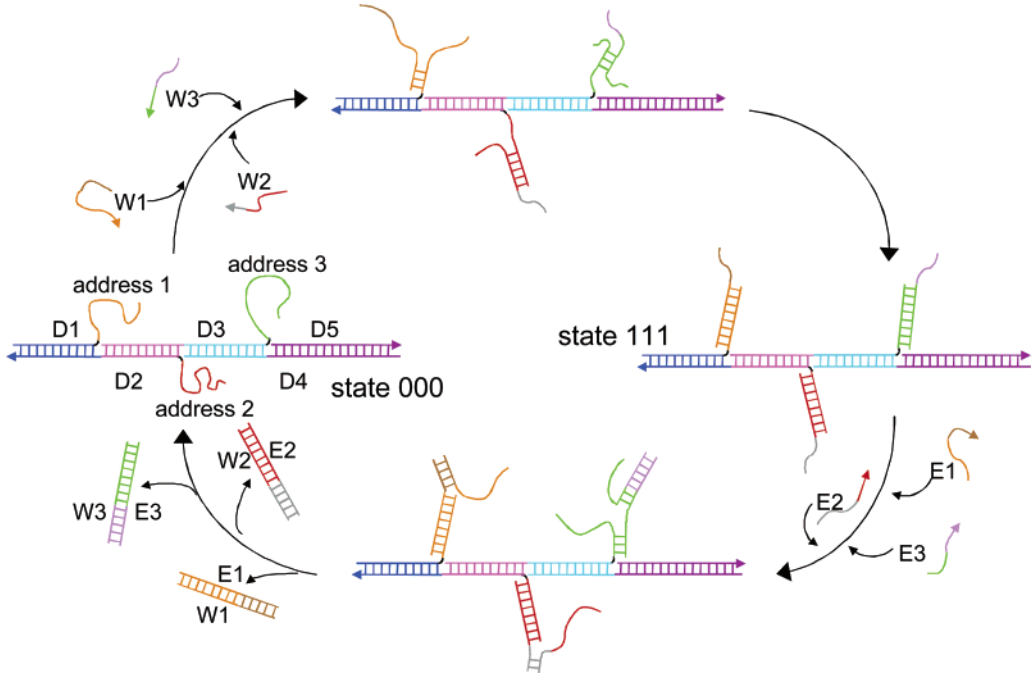

Figure 2. Operation cycle of the memory device. The drawings are colored as in Figure 1. The writing process is triggered by the addition of W strands, in which a W strand specifically associates with a cognate address branch. The addition of E strands resets the memory state by removing W strands from the device. The 10-base overhang on a W strand provides a toe-hold for the initiation of the branch migration that eventually leads to the hybridization of W and the cognate E strand, completing the erasure of that bit. The drawing shows a toggling between 000 (all "off") and 111 (all "on") states. Arrows in strand schematics represent the 3′ end.

Completion of the erasure event requires a branch migration to proceed until the E strand replaces the address branch in hybridizing to the W strand.

Sequential assembly of D strands is visualized by nondenaturing gel electrophoresis (Figure 3A), where formation of less mobile species illustrates a stepwise association of complementary segments. Address branches protruding from the double-stranded scaffold dramatically decrease the mobility of the device; a fully assembled device has 90 base pairs (state 000 in Figure 2), but gel electrophoresis shows an estimated length of 380 bp (lane 2 in Figure 3B). Ferguson analysis confirms that single-stranded branches greatly increase the effective molecular radius of the duplex backbone (see Table S1 and Figure S1 in Supporting Information). Sequence design is performed to avoid interactions between noncomplementary segments; no hybridization complexes between noncomplementary D strands are detected (see Figure S2 in Supporting Information). Although base-pairing of complementary strands can sometimes lead to the formation of dimers,[10] the present design does not admit this possibility. This expectation is supported by the results of Figure S3 in Supporting Information, demonstrating that varying the concentration of the memory device does not affect gel mobility or cause band splitting.

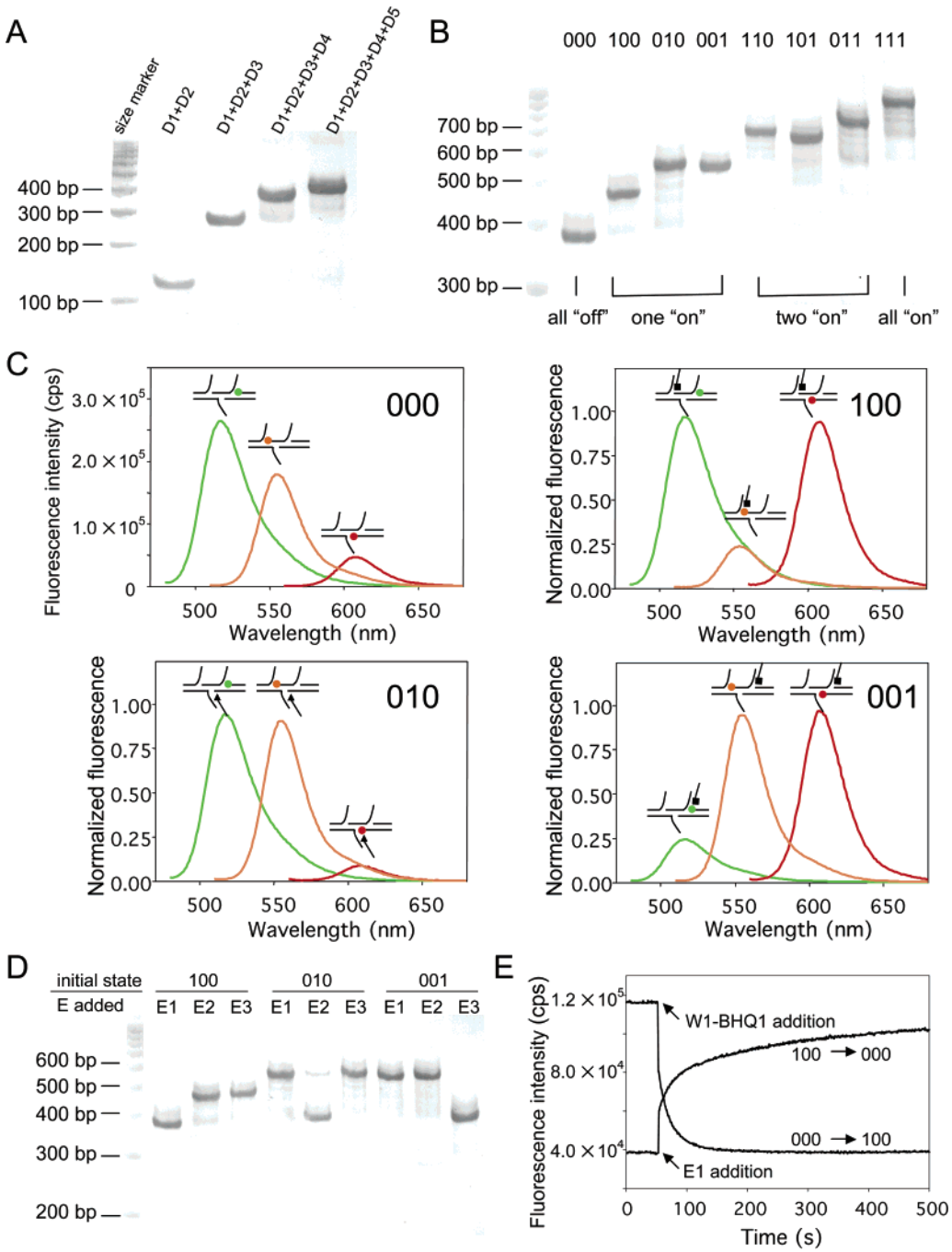

Figure 3. Analysis of device feasibility using gel electrophoresis and fluorescence. (A) Sequential device formation. (B) Gel electrophoresis of eight different memory states. (C) Verification of specific writing operations by fluorescence measurements. The solid lines in each figure are emission spectra for three devices exhibiting the same memory state but containing a different fluorescent label. Excitation for the different devices containing Ore (green circle in inset drawings), Hex (orange circle), or Tex (red circle) was performed at 470 nm (green line), 500 nm (orange line), or 550 nm (red line), respectively. The black square and triangle in inset drawings represent BHQ1 and Iowa Black, respectively. The spectra of states 100, 010 and 001 were normalized by the corresponding spectrum of state 000. (D) Specific erasing of the device. (E) Typical kinetic traces for the writing and erasing processes under pseudo-first-order reaction conditions. BHQ1-labeled W1 or E1 (final concentration = 100 nM) was added to 10 nM device containing Hex-labeled D3 and the solution was mixed by rapid pipetting. Excitation and emission wavelengths were 538 and 555 nm with 5 nm bandwidths.

To demonstrate accessibility of the address branches, all possible states of the device are prepared by adding equimolar W strands to the fully "off" device in state 000 (see Figure 3B). Hybridization of address branches with cognate W strands results in a low-mobility gel band, and the mobility is roughly inversely proportional to the number of addresses switched "on". States carrying the same number of "on" addresses show different mobilities (lanes 3−5 and 6−8), indicating different local environments for the addresses. The fully "on" device in state 111 has 144 base pairs (lane 9) but exhibits the mobility of a 900-bp helix, owing to the retarding effects of the 18-bp duplex branches.

The altered gel mobility (Figure 3B) does not provide direct evidence of specific addressing by W strands. Thus,

we employed fluorescence measurements to independently monitor the bit state of each address. The 5′ end of D3 is labeled with hexachlorofluorescein (Hex), the 3′ end of D4 is labeled with Texas Red (Tex) and the 5′ end of D5 is labeled with Oregon Green 488 (Ore). To prevent ambiguous interpretation of the fluorescence signal caused by fluorescence resonance energy transfer between dyes, three 000 devices, each containing a different dye, were prepared by mixing one of the fluorescent strands and the other four nonlabeled strands. Each fluorescent dye is in the vicinity of the 3-base spacer of a preceding address branch so the dye fluorescence can be quenched by a quencher-labeled W strand (e.g., Hex of D3 is quenched by W1). To this end, ends of W strands proximal to the 3-base spacer are labeled with a quencher, i.e., the 3′ ends of W1 and W3 with Black Hole Quencher-1 (BHQ1) and the 5′ end of W2 with Iowa black (see the inset drawings of Figure 3C). Using the fluorescent devices and the quencher-labeled W strands, readout of the memory state is performed by analyzing an emission spectrum of each dye as shown in Figure 3C. Three fluorescence peaks centered at 518, 555, and 608 nm are the emissions from Ore, Hex, and Tex and reflect the bit state of address 3, 1, and 2, respectively. The emission spectra for the memory states carrying one "on" address clearly demonstrate that W strands specifically hybridize with a cognate address. Dye quenching by a cognate W strand resulted in reduction of fluorescence intensity to 23% for Hex at address 1, 8% for Tex at address 2, and 24% for Ore at address 3, whereas the fluorescence intensity remained above 90% in the presence of a noncognate W strand hybridized with a remote address branch. It is also important to be able to specifically erase each "on" address to permit reuse of the memory. Figure 3D shows that only the cognate E strand can strip off the W strand from the device and restore the corresponding address to the "off" state.

The independence of each address during writing and erasing is critical for use in integrated applications. We address this issue by examining the hybridization kinetics for each address under pseudo-first-order reaction conditions where the W or E strand is in excess over the device. The writing process exhibits single-exponential kinetic traces whereas the erasing process shows double-exponential behavior (Figure 3E). The apparent writing rate constants obtained by curve fitting with a single exponential showed a linear dependence on W strand concentration (see Figure S4A in Supporting Information). The writing rate constant for address 1 of the state 000 ($k_{W1,000}$) obtained by a linear regression is 4.5×10^5 s^{-1} M^{-1}. The bit states of the other addresses do not affect the rate constant of address 1 (i.e., $k_{W1,010}$, $k_{W1,001}$, and $k_{W1,011}$ are nearly identical to $k_{W1,000}$); the same behavior is observed for addresses 2 and 3. These results indicate that the writing process proceeds independently of the previous memory state. The insensitivity of the writing process to possible steric hindrance by local structural complexity is consistent with the fact that the writing rate constant is in a typical range of association rate constants (10^5∼10^7 s^{-1} M^{-1}) for hybridization between short single-stranded oligonucleotides (6∼14-mer).[23] Although steric

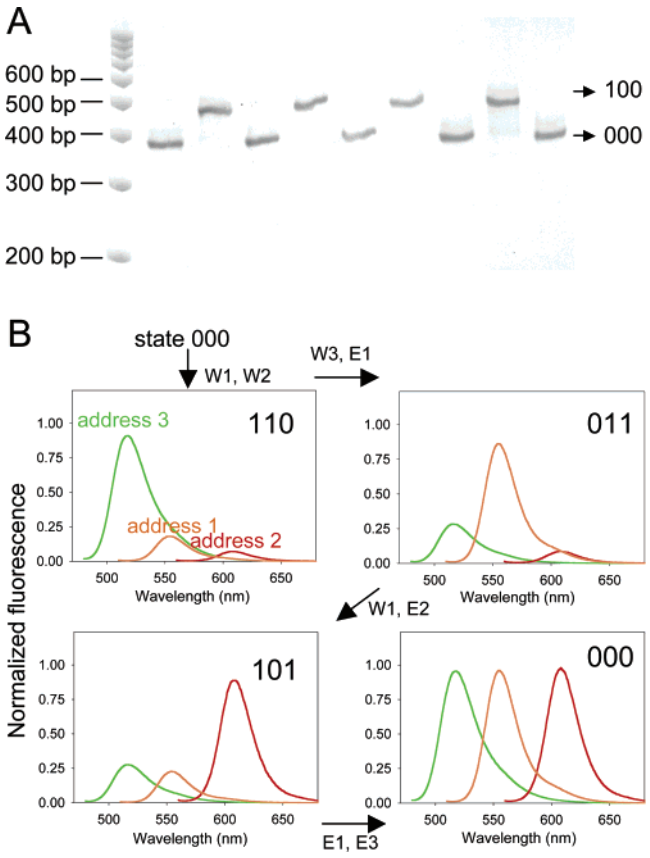

Figure 4. Cycling of the memory device. (A) Flipping between 000 and 100 states. Starting from state 000, the writing and erasing of address 1 was repeated four times by successively adding equimolar amounts of W1 or E1. (B) Multistate toggling. The spectra were normalized by the corresponding spectrum in the initial 000 state.

hindrance is not important for the writing process, the sequence composition of the address branch significantly affects the writing kinetics. The writing rate constants for addresses 2 and 3 are 5.9×10^5 and 2.0×10^5 s^{-1} M^{-1}, respectively. In contrast to the writing process, the erasing process exhibits double-exponential kinetic traces in which rate constants for the fast phase show a linear correlation to E strand concentration, whereas those for the slow phase are independent of the concentration variation (see Figure S4B in Supporting Information). The rate constants for the fast phase are 3.6×10^5, 5.2×10^4, and 1.7×10^5 s^{-1} M^{-1}, and those for the slow phase are 2.6×10^{-3}, 7.8×10^{-4}, and 1.3×10^{-3} s^{-1} for addresses 1, 2, and 3. The rate constants for the fast and slow phases are again independent of the previous memory state.

To investigate whether the device is capable of successive cycles, we first undertake four shuttling cycles between the 000 and 100 states (Figure 4A). Writing and erasing are carried out separately in each cycle and the device performance does not deteriorate as the cycle number increases. Multistate toggling of the global memory state is carried out by simultaneous writing and erasing, and the memory state is monitored by emission scans (Figure 4B). The fluorescence spectra of the restored 000 state after four successive state changes are nearly identical to those of the initial 000 state.

Figure 4 demonstrates that the device functions robustly as rewritable memory.

Memory state changes are based on specific molecular binding events spontaneously driven by free energy minimization, so no external energy source is required to preserve memory states and no sophisticated circuitry is required for random access. Although we consider a prototype array of three addresses, the number and spacing of the addresses may be easily adjusted. A one-dimensional device carrying N addresses achieves 2^N different states, and can be constructed using $N + 2$ DNA strands of moderate length (for oligonucleotide synthesis). If N is increased sufficiently, the conformational flexibility of the device scaffold will cause undesirable interactions between remote addresses. Immobilization of addresses on a more rigid two-dimensional lattice (e.g., those made of DNA[7−9] or protein[24]) may provide an attractive alternative for constructing high-density memory suitable for external readout by atomic force microscopy.[7,8,25] The controllable nanopatterning capability illustrated by the present DNA device may also be directly applied to molecular transport, propagating cargo through an array of address branches.

Acknowledgment. We wish to thank S. L. Mayo for comments on the manuscript. The following research support is gratefully acknowledged: DARPA and the Air Force Research Laboratory under agreement F30602-01-2-0561, the Ralph M. Parsons Foundation, and the Charles Lee Powell Foundation.

Supporting Information Available: Materials and methods. Ferguson analysis of device species. Kinetic analysis of the writing and erasing processes. Table S1: Ferguson analysis retardation coefficients. Figure S1: Ferguson plots of size markers and four device species. Figure S2: Formation of hybridization complexes between D strands. Figure S3: Nondenaturing PAGE with varying concentration of memory device. Figure S4: Concentration dependence of observed rate constants for writing and erasing processes at address 1. This material is available free of charge via the Internet at http://pubs.acs.org.

References

(1) Whitesides, G. M.; Grzybowski, B. *Science* **2002**, *295*, 2418−2421.
(2) Seeman, N. C. *Nature* **2003**, *421*, 427−431.
(3) Storhoff, J. J.; Mirkin, C. A. *Chem. Rev.* **1999**, *99*, 1849−1862.
(4) Seeman, N. C. *J. Theor. Biol.* **1982**, *99*, 237−247.
(5) Kallenbach, N. R.; Ma, R.-I.; Seeman, N. C. *Nature* **1983**, *305*, 829−831.
(6) Chen, J.; Seeman, N. C. *Nature* **1991**, *350*, 631−633.
(7) Winfree, E.; Liu, F.; Wenzler, L. A.; Seeman, N. C. *Nature* **1998**, *394*, 539−544.
(8) Yan, H.; LaBean, T. H.; Feng, L.; Reif, J. H. *Proc. Natl. Acad. Sci. U.S.A.* **2003**, *100*, 8103−8108.
(9) LaBean, T. H.; Yan, H.; Kopatsch, J.; Liu, F.; Winfree, E.; Reif, J. H.; Seeman, N. C. *J. Am. Chem. Soc.* **2000**, *122*, 1848−1860.
(10) Yurke, B.; Turberfield, A. J.; Mills, A. P., Jr.; Simmel, F. C.; Neumann, J. L. A. *Nature* **2000**, *406*, 605−608.
(11) Yan, H.; Zhang, X.; Shen, Z.; Seeman, N. C. *Nature* **2002**, *415*, 62−65.
(12) Mao, C.; Sun, W.; Shen, Z.; Seeman, N. C. *Nature* **1999**, *395*, 144−146.
(13) Alberti, P.; Mergny, J.-L. *Proc. Natl. Acad. Sci. U.S.A.* **2003**, *100*, 1569−1573.
(14) Benenson, Y.; Paz-Elizur, T.; Adar, R.; Keinan, E.; Livneh, Z.; Shapiro, E. *Nature* **2001**, *414*, 430−434.
(15) Mao, C.; LaBean, T. H.; Reif, J. H.; Seeman, N. C. *Nature* **2000**, *407*, 493−496.
(16) Braich, R. S.; Chelyapov, N.; Johnson, C.; Rothemund, P. W. K.; Adleman, L. *Science* **2002**, *296*, 499−502.
(17) Liu, Q.; Wang, L.; Frutos, A. G.; Condon, A. E.; Corn, R. M.; Smith, L. M. *Nature* **2000**, *403*, 175−179.
(18) Stojanovic, M.; Stefanovic, D. *Nature Biotech.* **2003**, *21*, 1069−1074.
(19) Alivisatos, A. P.; Johnsson, K. P.; Peng, X.; Wilson, T. E.; Loweth, C. J.; Bruchez, M. P.; Schultz, P. G. *Nature* **1996**, *382*, 609−611.
(20) Mirkin, C. A.; Letsinger, R. L.; Mucic, R. C.; Storhoff, J. J. *Nature* **1996**, *382*, 607−609.
(21) Hasty, J.; McMillen, D.; Collins, J. J. *Nature* **2002**, *420*, 224−230.
(22) Protozanova, E.; Macgregor, R. B., Jr. *Biochemistry* **1996**, *35*, 16638−16645.
(23) Turner, D. H. In *Nucleic Acids: Structures, Properties, and Functions*; Bloomfield, V. A., Crothers, D. M., Tinoco, I., Jr., Eds.; University Science Books: Sausalito, CA, 2000; pp 259−334.
(24) Shenton, W.; Pum, D.; Sleytr, U. B.; Mann, S. *Nature* **1997**, *389*, 585−587.
(25) Cavallini, M.; Biscarini, F.; Léon, S.; Zerbetto, F.; Bottari, G.; Leigh, D. A. *Science* **2003**, *299*, 531.

NL049658R